

# An Extensionally Fractured Upper Lithosphere on Io

Paul K. Byrne<sup>1</sup>, Rosaly Lopes<sup>2</sup>, Jani Radebaugh<sup>3</sup>, and David A Williams<sup>4</sup>

<sup>1</sup>Washington University in St. Louis

<sup>2</sup>Jet Propulsion Lab (NASA)

<sup>3</sup>Department of Geosciences

<sup>4</sup>Arizona State University

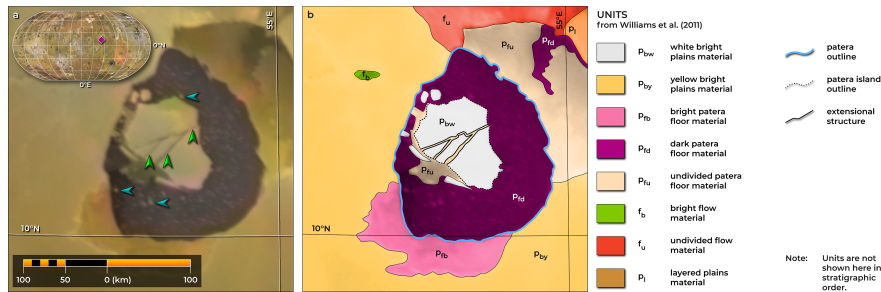
December 21, 2022

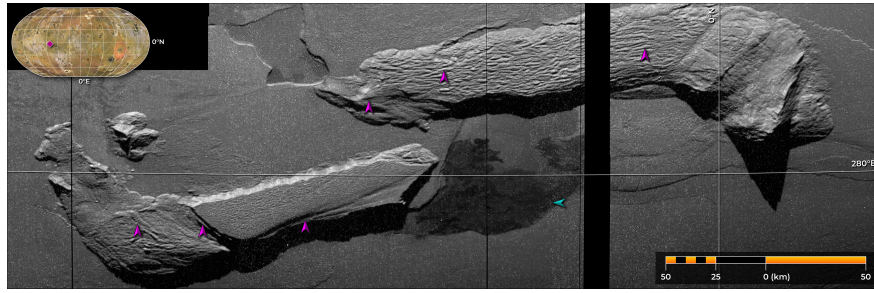
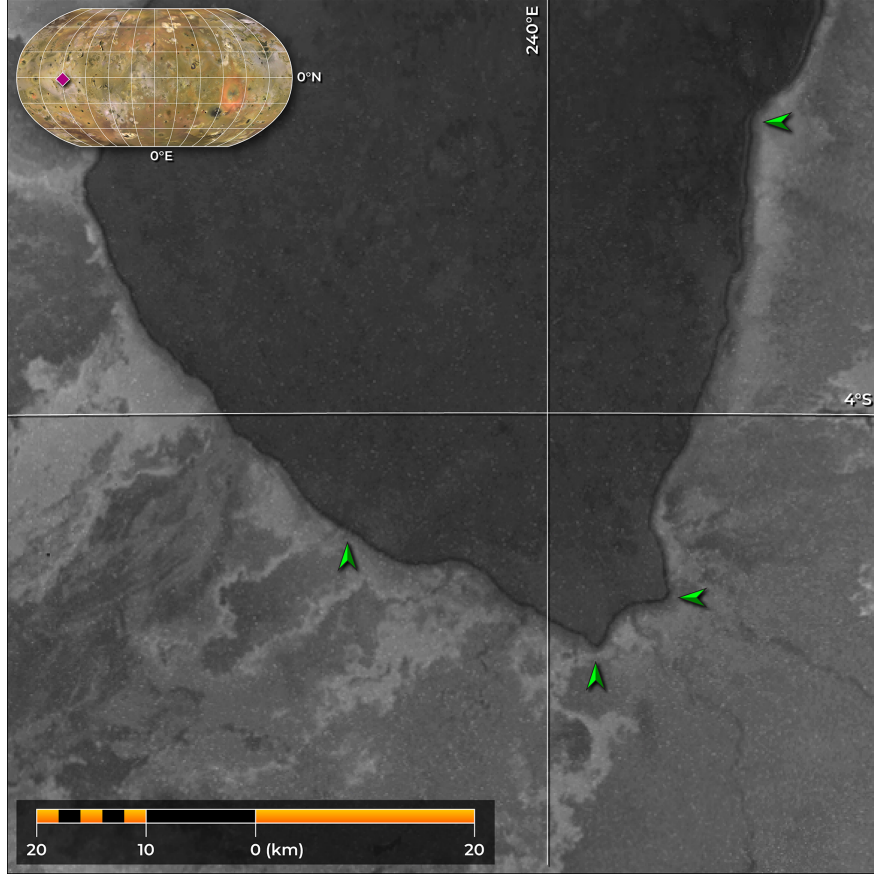
## Abstract

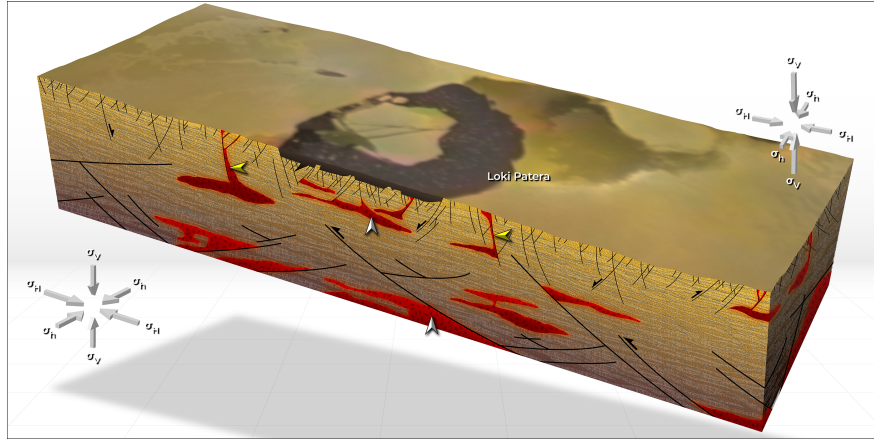
The Jovian moon Io features hundreds of paterae, broad depressions often filled with lava. The largest such example, Loki Patera, features a large, polygonal, and fractured island in its center. This island may reflect the fragmentation of the upper Ionian lithosphere by a shallow magma body, facilitated by a great number of shallow extensional structures. We propose a model for the Ionian lithosphere in which the upper portion is heavily deformed by joints, normal faults, and graben resulting from combined tidal, subsidence, and thermal stresses, and a lower portion rife with major thrust faults formed by horizontal compression of deeper crustal levels from the continued burial of surface units. Some of those thrusts may be reactivated normal faults. An extensionally fractured upper lithosphere accounts for the Loki Patera island, for observations of more than 175 paterae with straight edges, for the fact that almost 95% of Io's surface is covered with volcanic flow and plains units, and for widespread instances of mass wasting within Io's gigantic mountain blocks. Additional, high-resolution image and topographic data are required to test this hypothesized model for the moon's lithosphere.

## Hosted file

952345\_0\_art\_file\_10546126\_rn3yfp.docx available at <https://authorea.com/users/538926/articles/614202-an-extensionally-fractured-upper-lithosphere-on-io>







# An Extensionally Fractured Upper Lithosphere on Io

Paul K. Byrne<sup>1\*</sup>, Rosaly M. C. Lopes<sup>2</sup>, Jani Radebaugh<sup>3</sup>, and David A. Williams<sup>4</sup>

<sup>1</sup>Washington University in St. Louis, St. Louis, MO 63130, USA.

<sup>2</sup>Jet Propulsion Laboratory, California Institute of Technology, Pasadena, CA 91109, USA.

<sup>3</sup>Brigham Young University, Provo, UT 84602, USA.

<sup>4</sup>Arizona State University, Tempe, AZ 85287, USA.

\*Corresponding author: Paul Byrne ([paul.byrne@wustl.edu](mailto:paul.byrne@wustl.edu))

## Key Points:

- A distinctive polygonal “island” in Io’s largest patera may be a fractured crustal block
- There are numerous other indicators for a pervasively fractured Ionian lithosphere
- We propose a lithospheric model for Io with major shortening and extensional tectonics in the lower and upper portions, respectively

**25 Abstract**

26 The Jovian moon Io features hundreds of paterae, broad depressions often filled with lava. The largest  
27 such example, Loki Patera, features a large, polygonal, and fractured island in its center. This island  
28 may reflect the fragmentation of the upper Ionian lithosphere by a shallow magma body, facilitated by  
29 a great number of shallow extensional structures. We propose a model for the Ionian lithosphere in  
30 which the upper portion is heavily deformed by joints, normal faults, and graben resulting from  
31 combined tidal, subsidence, and thermal stresses, and a lower portion rife with major thrust faults  
32 formed by horizontal compression of deeper crustal levels from the continued burial of surface units.  
33 Some of those thrusts may be reactivated normal faults. An extensionally fractured upper lithosphere  
34 accounts for the Loki Patera island, for observations of more than 175 paterae with straight edges, for  
35 the fact that almost 95% of Io's surface is covered with volcanic flow and plains units, and for  
36 widespread instances of mass wasting within Io's gigantic mountain blocks. Additional, high-resolution  
37 image and topographic data are required to test this hypothesized model for the moon's lithosphere.

38

**39 Plain Language Summary**

40 Io is a large moon of Jupiter, and one of the most volcanically active bodies in the Solar System. Io has  
41 a distinctive landform type called "paterae" ("patera" in singular form), which are essentially large  
42 depressions filled with lava. The biggest patera is called Loki Patera, and in its middle is a polygonal  
43 island. We interpret this island as a fractured block of Io's crust. If this interpretation is correct, then it  
44 is possible that much of the upper portion of Io's crust is riddled with extensional fractures caused by  
45 several overlapping processes. A huge number of extensional fractures explains other aspects of Io's  
46 geology, such as the fact that almost half of all the moon's paterae have straight edges—which is  
47 something we'd expect to happen if paterae form in a heavily extensionally fractured crust. Io also has  
48 gigantic mountains, which are formed by compression of the lower crust as tremendous amounts of

49 lava erupt and bury everything around them. But even those mountains show lots of extensional  
50 tectonic structures, which provide further support for our idea about Io's crust.

51

## 52 **1 Introduction**

53 Jupiter's rocky moon Io is replete with towering mountain blocks (Schenk et al., 2001) and lava flows  
54 that cover virtually the entire surface (McEwen et al., 1998; Williams et al., 2011). Internal heat energy  
55 is principally supplied by tidal interactions with Jupiter and its neighboring moons (Peale et al., 1979).  
56 Chief among the satellite's most notable landforms are the paterae, broad depressions that are  
57 widespread and commonly filled with lavas (Radebaugh et al., 2001).

58 First described by Carr et al. (1979), paterae (*sing.* patera) are quasi-circular, shallow depressions  
59 with curved, straight, or scalloped edges. These landforms may be the Ionian equivalent to the calderas  
60 seen on Earth, Venus, and Mars, but a formation via collapse into a subsurface void space—the  
61 principal means by which calderas form (Lipman, 1997)—has yet to be confirmed for Io's paterae.  
62 Radebaugh et al. (2001) identified at least 417 paterae (425 including nested features: Williams et al.,  
63 2011) distributed across the ~80% of Io imaged at 2 km/pixel or better, with diameters ranging from  
64 2.5 to 202.6 km.

65 That largest patera is Loki, situated in Io's eastern hemisphere. Loki Patera features a prominent  
66 "island" in its center (Lopes-Gautier et al., 2000). Dark lines that cross this island are suggestive of  
67 tectonic lineaments—raising the possibility that the island is a fractured crustal block. If so, then the  
68 break-up of this block may offer valuable insights into the properties and tectonic state of Io's  
69 lithosphere.

70

## 71 **2 The Loki Patera Island**

72 Seen with combined data from the Voyager 1 Imaging Science Subsystem narrow-angle camera and  
73 the Galileo Solid-State Imaging System (SSI) camera (Figure 1a), the island is distinctly polygonal in

74 outline and measures approximately  $115 \times 110$  km in spatial extent along its north–south and east–west  
75 axes, respectively. A prominent lineament about 85 km long strikes east–northeast across the island,  
76 with two additional linear features (55 and 30 km long, respectively) striking to the northeast and  
77 abutting the first. Each of these features is  $\sim 2$ –3 km across. Smaller polygonal “islands” are present to  
78 the northwest and southwest of the larger block, and the dark patera floor is dotted with bright spots  
79 (termed “bergs”) that may be locally high-standing topography and/or surface deposits (Howell et al.,  
80 2013).

81 The morphology of these lineaments strongly suggests that they are extensional tectonic structures.  
82 Although lava flows can be much longer than they are wide, they tend to show digitate ends and widen  
83 with distance from their source vents (e.g., Carr et al., 1977) and so are not morphologically consistent  
84 with the Loki Patera island lineaments. Neither are other geological landforms that can have relatively  
85 linear planforms, such as mass-wasting deposits nor secondary crater chains (of which no examples are  
86 yet known for Io). Dikes often have straight margins that extend for tens of kilometers or more, but on  
87 that scale are bounded by steep, near-vertical fractures (e.g., Ernst et al., 2001). We therefore interpret  
88 these lineaments as being extensional in nature, either tensile fractures (i.e., joints) or, more likely  
89 given their scale, are paired, antithetic, inward-dipping normal faults (i.e., graben).

90 Near-Infrared Mapping Spectrometer data returned by the Galileo mission indicate that both the  
91 patera floor and the material within these fractures are warmer than the island and the plains  
92 surrounding the patera (Lopes-Gautier et al., 2000); these thermal characteristics are shared by many  
93 other paterae on Io (Radebaugh et al., 2001). Per our reasoning, the Loki Patera island is in fact several  
94 discrete (but formerly contiguous) blocks that have rafted apart in a manner akin to pack ice, and the  
95 material between the blocks is the lava that covers the entire patera floor. Comparison of image data of  
96 Loki Patera from the Galileo and Voyager missions indicate that the island and its constituent fractures  
97 show no resolvable change in position or size over the intervening two decades (Lopes-Gautier et al.,  
98 2000). Moreover, the kinetic and thermal effects of two concurrent resurfacing “waves” observed in

99 March 2015 did not appear to disrupt or destroy the island, strongly indicating that this feature has  
100 persisted for at least the 36 years since its discovery in 1979, and that it may now be sitting on, or is  
101 anchored to, the patera floor (de Kleer et al., 2017).

102

### 103 **3 Implications for Ionian Volcanotectonics**

#### 104 *3.1 Patera Formation*

105 As large, irregular depressions overwhelmingly associated with lava flows, paterae have been  
106 interpreted as the Ionian counterparts to calderas on Earth, Venus, and Mars (e.g., Carr et al., 1979).  
107 Yet calderas on those worlds are generally characterized by quasi-circular or arcuate outlines  
108 (Crumpler et al., 1996) and peripheral zones of crustal extension (Walter and Troll, 2011), and are  
109 frequently associated with voluminous deposits of lava, ash, or both (Lipman, 1997). Indeed, 42% of  
110 the 417 paterae surveyed by Radebaugh et al. (2001) have straight or irregular margins that terminate at  
111 sharp corners (e.g., Figure 2). Adjacent extensional structures are not commonly observed, although  
112 this dearth of extensional tectonics may be a function of available image resolution and Io's prodigious  
113 global resurfacing rate of ~1.5 cm/yr (Kirchoff and McKinnon, 2009). And no volcanic deposits of  
114 sufficient volume to match the observed depression have been unequivocally recognized proximal to,  
115 and having come from, any patera (Keszthelyi et al., 2004).

116 Paterae may instead be the result of the stalling of silicate magma at shallow depths that undermines  
117 the overlying crust, particularly if that crust is SO<sub>2</sub> rich and porous (Keszthelyi et al., 2004). Under this  
118 scenario, the heat from an intrusion melts sulfur and/or SO<sub>2</sub>, which mobilizes into the surrounding  
119 country rock and leaves behind pore space. With continued melting, a substantial depression forms or  
120 the magma chamber can even be fully unroofed (Keszthelyi et al., 2004). By this view, Io's paterae  
121 differ from conventional calderas by forming not because of the eruption or lateral withdrawal of  
122 magma but by the migration of volatiles through a crust that becomes increasingly porous or otherwise  
123 mechanically weak (cf. Kargel et al., 1999).

124       Regardless of the means of collapse, the disruption of a magma chamber roof would be readily  
125 enhanced by pre-existing extensional fractures in the crust—such as those that cross the Loki Patera  
126 island. We infer that these structures predate the formation of Loki Patera for two reasons: a) they do  
127 not have a spatial distribution or arrangement consistent with extensional strains associated with  
128 magma chamber tumescence or collapse (e.g., Walter and Troll, 2001); and b) at tens of km long, their  
129 dimensions are comparable to the lengths of those portions of other paterae margins that are straight  
130 and have been interpreted to reflect tectonic control (e.g., Radebaugh et al., 2001).

131       It may be, then, that the island is a remnant of fractured crust that overlaid and foundered into a  
132 shallow, stalled magma body. The rest of the roof material might even have been subsumed by lava  
133 entirely, accounting for why there are few similar, fractured islands in other paterae. (Some other  
134 paterae have islands, such as the 28 km-diameter Steropes Patera (Radebaugh et al., 2001) or the 75  
135 km-wide Tupan Patera (Black, 2006), but available image data are insufficient to survey all such  
136 examples on Io, or determine how many, if any, are also fractured.) Further, should the Loki block be  
137 sitting on the patera floor, sufficiently anchored so as to remain seemingly stationary at least since its  
138 first observation in 1979 (de Kleer et al., 2017), then it follows that as a result of the creation of void  
139 space in the subsurface, the block’s upper surface should be lower than the surrounding plains. Lava  
140 from floor eruptions could then exploit and undermine fractures in the island to thermally erode and  
141 enlarge them, such that those structures become visible at Voyager image resolutions.

142

### 143 *3.2 Fracturing of the Ionian Upper Lithosphere*

144       The fractured block in Loki, the finding of almost half of all paterae having straight margins, and the  
145 fact that some patera walls are steep and stand kilometers tall—such as the margins of Chaac Patera,  
146 which are 2.7 km high and have slopes of 70° (Radebaugh et al., 2001)—together imply strong tectonic  
147 control on the formation of at least some paterae. Certainly *thrust* faults are widespread on Io, with the  
148 straight margins of many of the moon’s enormous mountain blocks (Figure 3) taken as evidence of

149 shortening tectonics, attributed to subsidence of the crust under continually emplaced lavas (Schenk  
150 and Bulmer, 1998; Turtle et al., 2001).

151 But there are reasons to expect substantial *extensional* deformation of the upper Ionian lithosphere,  
152 too. For example, temporally and spatially localized decreases in eruptive activity, set against a  
153 backdrop of sustained tidal heating, are predicted to generate considerably large, horizontally  
154 compressive stresses deep in the Ionian crust, but horizontally extensional stresses near the surface  
155 (McKinnon et al., 2001; Kirchoff et al., 2020). Similarly, the formation of Io's gigantic mountain  
156 blocks along deep-seated thrust faults is thought to be accompanied by widespread extension and the  
157 formation of normal faults and graben (Bland and McKinnon, 2016). Some of these extensional  
158 structures may penetrate as much as 15 km into the footwall (Bland and McKinnon, 2016)—consistent  
159 with the great heights and slope angles of, for instance, the Chaca Patera walls. Extensional fractures  
160 would efficiently conduct ascending magma to the surface (Bland and McKinnon, 2016; McGovern et  
161 al., 2016; Byrne et al., 2018), allowing magma to erupt that would otherwise be too dense to avoid  
162 stalling in the shallow crust (Keszthelyi et al., 2004). At least some of these extensional structures have  
163 a dip component of slip (Ahern et al., 2017).

164 Even within the uplifted and tilted mountain blocks, there is considerable extensional deformation,  
165 such as the scarp-parallel lineaments on the back scarps of the Hi'iaka Montes (Ahern et al., 2017)  
166 (Figure 3). Similarly, Schenk and Bulmer (1998) documented landslide scarps on Euboea Montes—  
167 presumably great listric normal faults, on the basis of comparisons with landslide deposits on Earth and  
168 other planets (e.g., Lopes et al., 1980; Riley et al., 1999).

169

#### 170 **4 Discussion**

171 A highly extensionally deformed upper, brittle lithosphere accounts for several separate but related sets  
172 of observations of Io.

173 Firstly, the prevalence of such structures explains why the central island in Loki Patera has a  
174 polygonal outline and appears dissected by fractures: the island is a formerly coherent block that broke  
175 apart along pre-existing fractures atop a shallow magma body as that body (and the patera) grew, by the  
176 withdrawal and/or eruption of magma, via the mobilization of sulfur-bearing volatiles (Keszthelyi et  
177 al., 2004), or by a combination of these processes. In any case, since *some* subsurface material was  
178 removed, that central island must now be at a lower elevation than the surrounding plains and is  
179 perhaps sitting on the patera floor. The smaller islands and bergs in Loki may be other, smaller  
180 fragments of the original chamber roof, consistent with the view of Howell et al. (2013) that such  
181 features are not concentrations of sulfur deposits but are instead isolated areas of terrain that avoided  
182 burial by subsequent lavas. It is not clear why the large island has remained intact, in contrast to some  
183 of the smaller fragments throughout the patera floor (Howell et al., 2013), although there may well be a  
184 resolution effect at play since those smaller fragments visible in Voyager images are not resolved with  
185 Galileo data. The island may simply be the largest remaining piece of an ongoing process that will  
186 ultimately destroy the original roof over the magma body entirely, in which case Loki will eventually  
187 come to resemble other paterae where no large islands are present—and, by implication, other paterae  
188 may once have had large island fragments.

189 Secondly, widespread joints and normal faults in the crust account for the straight margins of a  
190 substantial number of Io's paterae (Radebaugh et al., 2001), with these structures forming the  
191 boundary(ies) of patera(e) as shallow magma bodies undermined and drove the collapse of the  
192 overlying, fractured roof material (Keszthelyi et al, 2004). The numerous instances of sharp paterae  
193 corners noted by Radebaugh et al. (2001) might reflect the tectonic influence of intersecting sets of  
194 joints or normal faults. Moreover, the extension associated with the mountain formation models of  
195 Bland and McKinnon (2016) and Kirchoff et al. (2020) is consistent with the finding that paterae—  
196 assuming their form is controlled by pre-existing normal faults—are much more commonly collocated  
197 with mountains than predicted by chance alone (Radebaugh et al. 2001; Jaeger et al., 2003).

198 Thirdly, abundant extensional structures provide ready conduits for magma to reach the surface;  
199 indeed, the normal and transtensional fractures that characterize an extensional tectonic regime are  
200 more conducive to magma ascent than reverse or transpressional fractures, given that crustal shortening  
201 results in negative horizontal elongation whereas horizontal extension opens vertical accommodation  
202 space into which magma can move (e.g., Byrne et al., 2018). A prevailing horizontally extensional  
203 tectonic regime in its upper lithosphere is thus compatible with Io being almost entirely covered by  
204 extensive lava flows and vast plains units, the latter of which mainly comprise buried lavas and  
205 pyroclastic deposits (McEwan et al., 2000; Williams et al., 2002). Indeed, plains and lava flow units  
206 occupy 66.6% and 27.8% of the surface, respectively (Williams et al., 2011).

207 Finally, Schenk and Bulmer (1998) proposed that uplifted blocks rise along deep-rooted thrust  
208 faults, drawing a parallel between Io's mountains and basement-cored uplifts in the western United  
209 States. In the latter case, those shortening structures moved along reactivated, high-angle normal faults  
210 that originally formed via crustal extension (e.g., Reches, 1978). For horizontal compression, incipient  
211 thrust faults form with low dip angles (Anderson, 1905). Therefore, should at least some mountain  
212 blocks be bounded by high-angle reverse faults as suggested by Ahern et al. (2017), then those  
213 bounding structures could have formed as normal faults that were later reactivated when horizontally  
214 compressive stresses built at the base of the lithosphere from sustained burial of surface materials  
215 (Bland and McKinnon, 2016).

216 We thus propose a model for Io whereby the upper lithosphere features a pervasive fracture network  
217 formed by a combination of tidal, subsidence, and thermal stresses—with large, deep-seated thrust  
218 faults and widespread normal faults dominant at lower and upper crustal levels, respectively (Figure 4).  
219 Abundant extensional structures at shallow crustal levels serve as failure planes along which  
220 undermined magma chamber roofs collapse, and are available for reactivation with a reverse or oblique  
221 sense of slip if favorably aligned to local, subsequent stress fields. The apparent dearth of extensional  
222 strain (beyond paterae and mountain block edges) on Io is probably a function of the moon's

223 extraordinary volcanic resurfacing rate, which likely obscures just how deformed the near surface  
224 actually is.

225 This stress state is in marked contrast to other terrestrial bodies in the Solar System. For instance,  
226 although there are major thrust fault-related landforms on Mercury as is the case on Io, those on the  
227 innermost planet are interpreted to have formed from secular interior cooling (Strom et al., 1975; Byrne  
228 et al., 2018). The resulting horizontally compressive stress field results in a dearth of extensional  
229 structures at the surface, and inhibits the ascent of magma to shallow depths in all but the weakest parts  
230 of the planet's crust (Byrne et al., 2018). The tectonic characteristics of Mercury are largely shared by  
231 the Moon (e.g., Byrne, 2020). Venus and Earth are replete with both extensional and shortening  
232 landforms, although each is in a different tectonic regime than that of Io (e.g., Byrne, 2020; Lourenço  
233 et al. 2020). Mars, too, has widespread extensional tectonics (e.g., Byrne, 2020), attributed at least in  
234 part to near-surface stresses associated with the Tharsis Rise (e.g., Anderson et al., 2001), as well as  
235 shortening structures reflecting both Tharsis-related loading stresses and global contraction (e.g., Nahm  
236 and Schultz, 2010). But none of the inner Solar System worlds has a tectonic inventory matching Io.

237 The Jovian moon is also distinctive among outer Solar System satellites in that it is the only such  
238 body without an icy exterior. Although tectonic structures including graben and thrust fault-related  
239 landforms are widespread on myriad other icy moons (e.g., Collins et al., 2010), none boasts the  
240 elevated mountain blocks nor visibly craterless surface of Io (Williams et al., 2011). Io's tectonic stress  
241 state is the result principally of its inordinate effusive volcanism, which in turn is driven by the  
242 dissipation of tidal energy in its interior (Peale et al., 1979). By this measure, Io's lithospheric stress  
243 state may be unique in the Solar System—but could be illustrative of tidally heated planets orbiting  
244 other stars (Barr et al., 2018; McEwen et al., 2020).

245

## 246 **5 Conclusions**

247 The distinctive, polygonal “island” in Loki Patera holds clues to Io’s lithospheric stress state. This  
248 island may be a fractured crustal block, the remains of a portion of the crust undermined by a shallow  
249 magma body aided by widespread extensional deformation. A heavily extensionally deformed upper  
250 lithosphere, likely by a combination of subsidence, tidal, and thermal stresses, accounts for several  
251 seemingly disparate observations, including:

- 252 1) The polygonal, fractured appearance of the Loki Patera island;
- 253 2) A substantial number of other paterae with straight edges;
- 254 3) A globally youthful surface; and
- 255 4) The extensional strains so commonly seen within Io’s enormous, uplifted mountains.

256 We therefore propose a scenario for Io under which the lower lithosphere is deformed by large,  
257 deep-seated thrust faults from the burial of surface materials, but that is also riven by extensional  
258 tectonics in the near surface.

259 The acquisition of image and topographic data at resolutions substantially greater than those  
260 returned by the Voyager and Galileo missions would enable the search for and measurements of joints,  
261 normal faults, and graben in the plains proximal to paterae and mountain blocks, and would also  
262 establish if the elevation of the upper surface of the island is in fact below that of the surrounding  
263 plains. Such data would also provide a valuable comparison for assessing whether the Loki island  
264 really has remained stationary since its discovery. Further, the detection of small-scale extensional  
265 structures undergoing burial by active volcanism would lend support to the hypothesis that the Ionian  
266 lithosphere is far more tectonically disrupted than previously recognized.

267

## 268 **Open Research**

269 No new data were created for this study. All Voyager and Galileo image data used in this paper are  
270 publicly available at the NASA Planetary Data System (PDS) at <https://pds.nasa.gov>. The  
271 photogeological data shown in Fig. 1a and used for preparing the structural sketch in Fig. 1b (and for

272 the surface texture of the block in Fig. 4) is the combined Voyager–Galileo SSI global 1 km/px mosaic,  
273 available at [https://astrogeology.usgs.gov/search/map/Io/Voyager-Galileo/Io\\_GalileoSSI-](https://astrogeology.usgs.gov/search/map/Io/Voyager-Galileo/Io_GalileoSSI-Voyager_Global_Mosaic_1km)  
274 [Voyager\\_Global\\_Mosaic\\_1km](https://astrogeology.usgs.gov/search/map/Io/Voyager-Galileo/Io_GalileoSSI-Voyager_Global_Mosaic_1km). The data used to generate Figs. 2 and 3 are from the Galileo Solid-State  
275 Imaging (SSI) dataset (Thaller, 2000).

276

## 277 **Acknowledgments**

278 Part of this research was conducted at the Jet Propulsion Laboratory, California Institute of  
279 Technology, under contract with NASA. This research made use of NASA’s PDS and Astrophysics  
280 Data System.

281

## 282 **References**

- 283 Ahern, A. A., Radebaugh, J., Christensen, E. H., Harris, R. A., & Tass, E. S. (2017), Lineations and  
284 structural mapping of Io’s paterae and mountains: Implications for internal stresses. *Icarus*, *297*, 14–  
285 32. doi:10.1016/j.icarus.2017.06.004.
- 286 Anderson, E. M. (1905), The dynamics of faulting. *Transactions of the Edinburgh Geological Society*,  
287 *8*(3), 387–402. doi:10.1144/transed.8.3.387.
- 288 Anderson, R. C., et al. (2001), Primary centers and secondary concentrations of tectonic activity  
289 through time in the western hemisphere of Mars. *Journal of Geophysical Research*, *106*, 20563–  
290 20585. doi:10.1029/2000JE001278.
- 291 Barr, A. C., Dobos, V., & Kiss, L. L. (2018), Interior structures and tidal heating in the TRAPPIST-1  
292 planets. *Astronomy and Astrophysics*, *613*, A37. doi:10.1051/0004-6361/201731992.
- 293 Black, S. R. (2006). *The origin and evolution of islands in Ionian paterae* (Master’s thesis). Retrieved  
294 from UMI ProQuest Digital Dissertations. (1436720). New York: State University of New York at  
295 Buffalo.

- 296 Bland, M. T., & McKinnon, W. B. (2016), Mountain building on Io driven by deep faulting. *Nature*  
297 *Geoscience*, 9, 429–433. doi:10.1038/NGEO2711.
- 298 Byrne, P. K, Whitten, J. L., Klimczak, C., McCubbin, F. M., & Ostrach, L. R. (2018), The volcanic  
299 character of Mercury. In Solomon, S. C., Nittler, L. R., and Anderson, B. J. (eds.), *Mercury: The*  
300 *View after MESSENGER*, 287–323. Cambridge University Press, Cambridge, UK.  
301 doi:10.1017/9781316650684.012.
- 302 Byrne, P. K. (2020) A comparison of inner Solar System volcanism. *Nature Astronomy*, 4, 321–327.  
303 doi:10.1038/s41550-019-0944-3.
- 304 Carr, M. H., Greeley, R., Blasius, K. R., Guest, J. E., & Murray, J. B. (1977), Some Martian volcanic  
305 features as viewed from the Viking Orbiters. *Journal of Geophysical Research*, 82, 3985–4015.  
306 doi:10.1029/JS082i028p03985.
- 307 Carr, M. H., Masursky, H., Strom, R. G., & Terrile, R. J. (1979), Volcanic features of Io. *Nature*, 280,  
308 729–733. doi:10.1038/280729a0.
- 309 Collins, G. C., et al. (2010), Tectonics of the outer planet satellites. In Watters, T. R., and Schultz, R.  
310 A. (eds.), *Planetary Tectonics*, Cambridge University Press, 264–350.
- 311 Crumpler, L. S., Head, J. W., & Aubele, J. C. (1996), Calderas on Mars: characteristics, structure, and  
312 associated flank deformation. In McGuire, W. J., Jones, A. P., and Neuberg, J. (eds.), *Volcano*  
313 *Instability on the Earth and Other Planets*, Geological Society Special Publication No. 110, 307–  
314 348.
- 315 de Kleer, K., Skrutskie, M., Leisenring, J., Davies, A. G., Conrad, A., de Pater, I., Resnick, A., Bailey,  
316 V., Defrère, D., Hinz, P., Skemer, A., Spalding, E., Vaz, A., Veillet, C., & Woodward, C. E. (2017),  
317 Multi-phase volcanic resurfacing at Loki. *Nature*, 545, 199–202. doi:10.1038/nature22339.
- 318 Ernst, R. E., Grosfils, E. B., & Mège, D. (2001), Giant dike swarms: Earth, Venus, and Mars. *Annual*  
319 *Review of Earth and Planetary Science*, 29, 489–534. doi:10.1146/annurev.earth.29.1.489.

- 320 Howell, R. R., Landis, C. E., & Lopes, R. M. C. (2013), Composition and location of volatiles at Loki  
321 Patera, Io. *Icarus*, 229, 328–339. doi:10.1016/j.icarus.2013.11.016.
- 322 Jaeger, W. L., Turtle, E. P., Keszthelyi, L. P., Radebaugh, J., & McEwan, A. S. (2003), Orogenic  
323 tectonism on Io. *Journal of Geophysical Research*, 108, E8, 5093. doi:10.1029/2002JE001946.
- 324 Kargel, J. S., Delmelle, P., & Nash, D. B. (1999), Volcanogenic sulfur on Earth and Io: Composition  
325 and spectroscopy. *Icarus*, 142, 249–280. doi:10.1006/icar.1999.6183.
- 326 Keszthelyi, L., Jaeger, W. L., Turtle, E. P., Milazzo, M., & Radebaugh, J. (2004), A post-Galileo view  
327 of Io's interior. *Icarus*, 169, 271–286. doi:10.1016/j.icarus.2004.01.005.
- 328 Kirchoff, M. R., & McKinnon, W. B. (2009), Formation of mountains on Io: Variable volcanism and  
329 thermal stresses. *Icarus*, 201, 598–614. doi:10.1016/j.icarus.2009.02.006.
- 330 Kirchoff, M. R., McKinnon, W. B., & Bland, M. T. (2020), Effects of faulting on crustal stresses  
331 during mountain formation on Io. *Icarus*, 335, 113326. doi:10.1016/j.icarus.2019.05.028.
- 332 Lipman, P. W. (1997), Subsidence of ash-flow calderas; relation to caldera size and magma-chamber  
333 geometry. *Bulletin of Volcanology*, 59, 198–218. doi:10.1007/s004450050186.
- 334 Lopes, R. M. C., Guest, J. E., & Wilson, C. J. (1980), Origin of the Olympus Mons aureole and  
335 perimeter scarp. *The Moon and Planets*, 22, 221–234. doi:10.1007/BF00898433.
- 336 Lopes-Gautier, R. M. C., Douté, S., Smythe, W. D., Kamp, L. W., Carlson, R. W., Davies, A. G.,  
337 Leader, F. E., McEwan, A. S., Geissler, P. E., Kieffer, S. W., Keszthelyi, L., Barbinis, E., Mehlman,  
338 R., Segura, M., Shirley, J., & Soderblom, L. A. (2000), A close-up look at Io from Galileo's near-  
339 infrared mapping spectrometer. *Science*, 288, 1201–1204. doi:10.1126/science.288.5469.1201.
- 340 Lourenço, D. L., Rozel, A. B., Ballmer, M. D., & Tackley, P. J. (2020), Plutonic-squishy lid: A new  
341 global tectonic regime generated by intrusive magmatism on Earth-like planets. *Geochemistry,*  
342 *Geophysics, Geosystems*, 21, e2019GC008756. doi:10.1029/2019GC008756.
- 343 McEwan, A. S., Keszthelyi, L., Spencer, J. R., Schubert, G., Matson, D. L., Lopes-Gautier, R. M. C.,  
344 Klaasen, K. P., Johnson, T. V., Head, J. W., Geissler, P., Fagents, S., Davies, A. G., Carr, M. H.,

- 345 Breneman, H. H., & Belton, M. J. S. (1998), High-temperature silicate volcanism on Jupiter's moon  
346 Io. *Science*, *281*, 87–90. doi:10.1126/science.281.5373.87.
- 347 McEwen, A. S., Belton, M. J. S., Breneman, H. H., Fagents, S. A., Geissler, P., Greeley, R., Head, J.  
348 W., Hoppa, G., Jaeger, W. L., Johnson, T. V., Keszthelyi, L., Klaasen, K. P., Lopes-Gautier, R. M.  
349 C., Magee, K. P., Milazzo, M. P., Moore, J. M., Pappalardo, R. T., Phillips, C. B., Radebaugh, J.,  
350 Schubert, G., Schuster, P., Simonelli, D. P., Sullivan, R., Thomas, P. C., Turtle, E. P., & Williams,  
351 D. A. (2000), Galileo at Io: Results from High-Resolution Imaging. *Science*, *288*, 1193–1198.  
352 doi:10.1126/science.288.5469.1193.
- 353 McEwen, A. S., et al. (2020), Tidal heating: Lessons from Io and the Jovian system; Relevance to  
354 exoplanets. *Exoplanets in our Backyard, 1*, abstract 3005.
- 355 McGovern, P. J., Kirchoff, M. R., White, O. L., & Schenk, P. M. (2016), Magma ascent pathways  
356 associated with large mountains on Io. *Icarus*, *272*, 246–257. doi:10.1016/j.icarus.2016.02.035.
- 357 McKinnon, W. B., Schenk, P. M., & Dombard, A. J. (2001), Chaos on Io: A model for formation of  
358 mountain blocks by crustal heating, melting, and tilting. *Geology*, *29*, 103–106. doi:10.1130/0091-  
359 7613(2001)029<0103:COIAMF>2.0.CO;2.
- 360 Nahm, A. L., & Schultz, R. A. (2010), Evaluation of the orogenic belt hypothesis for the formation of  
361 the Thaumasia Highlands, Mars. *Journal of Geophysical Research*, *115*, E04008.  
362 doi:10.1029/2009JE003327.
- 363 Peale, S. J., Cassen, P., & Reynolds, R. T. (1979), Melting of Io by tidal dissipation. *Science*, *203*, 892–  
364 894. doi:10.1126/science.203.4383.892.
- 365 Radebaugh, J., Keszthelyi, L. P., McEwan, A. S., Turtle, E. P., Jaeger, W. L., and Milazzo, M. (2001),  
366 Paterae on Io: A new type of volcanic caldera? *Journal of Geophysical Research*, *106*, 33,005–  
367 33,020. doi:10.1029/2000JE001406.

- 368 Reches, Z. (1978), Development of monoclines: Part I. Structure of the Palisades Creek branch of the  
369 East Kaibab monocline, Grand Canyon, Arizona. *Geological Society of America, Memoir 151*, 235–  
370 271. doi:10.1130/MEM151-p235.
- 371 Riley, C. M., Diehl, J. F., Kirschvink, J. L., & Ripperdan, R. L. (1999), paleomagnetic constraints on  
372 fault motion in the Hilina Fault System, south flank of Kilauea Volcano, Hawaii. *Journal of*  
373 *Geophysical Research*, 94, 233–249. doi:10.1016/S0377-0273(99)00105-5.
- 374 Schenk, P. M., & Bulmer, M. H. (1998), Origin of mountains on Io by thrust faulting and large-scale  
375 mass movements. *Science*, 279, 1514–1517. doi:10.1126/science.279.5356.1514.
- 376 Schenk, P. M., Hargitai, H., Wilson, R., McEwan, A., & Thomas, P. C. (2001), The mountains of Io:  
377 Global and geological perspectives from Voyager and Galileo. *Journal of Geophysical Research*,  
378 106, 33,201–33,222. doi:10.1029/2000JE001408.
- 379 Strom, R. G., Trask N. J., & Guest J. E. (1975), Tectonism and volcanism on Mercury. *Journal of*  
380 *Geophysical Research*, 80, 2478–2507. doi:10.1029/JB080i017p02478.
- 381 Thaller, T. F. (2000), Galileo orbital operations Solid State Imaging raw EDR v1.0 [Data set]. NASA  
382 Planetary Data System. doi:10.17189/1520425.
- 383 Turtle, E. P., Jaeger, W. L., Keszthelyi, L. P., McEwan, A. S., Milazzo, M., Moore, J., Phillips, C. B.,  
384 Radebaugh, J., Simonelli, D., Chuang, F., Schuster, P., & the Galileo SSI Team (2001), Mountains  
385 on Io: High-resolution Galileo observations, initial interpretations, and formation models. *Journal of*  
386 *Geophysical Research*, 106, 33,175–33,199. doi:10.1029/2000JE001354.
- 387 Walter, T. R., & Troll, V. R. (2001), Formation of caldera periphery faults: an experimental study.  
388 *Bulletin of Volcanology*, 63, 191–203. doi:10.1007/s004450100135.
- 389 Williams, D. A., Radebaugh, J., Keszthelyi, L. P., McEwen, A. S., Lopes, R. M. C., Douté, S., &  
390 Greeley, R. (2002), Geologic mapping of the Chaac-Camaxtli region of Io from Galileo imaging  
391 data. *Journal of Geophysical Research*, 107, E9, 5068. doi:10.1029/2001JE001821.

392 Williams, D. A., Keszthelyi, L. P., Crown, D. A., Yff, J. A., Jaeger, W. L., Schenk, P. M., Geissler, P.  
393 E., & Becker, T. L. (2011), Geologic map of Io: U.S. Geological Survey Scientific Investigations  
394 Map 3168, scale 1:15,000,000, 25 p., available at <https://pubs.usgs.gov/sim/3168/>.

395 **Figures**

396 **Figure 1.** Loki Patera. (a) Combined monochrome Voyager 1 and color Galileo imagery at 1 km/pixel.  
397 The floor of the patera is dark, in contrast to the brighter polygonal island. We infer the dark, linear  
398 features crossing the island (green arrows) as extensional tectonic structures. Smaller patches of bright  
399 material dot the patera floor (blue arrows). The location of Loki Patera is shown with a purple diamond  
400 on the global Io mosaic (in Robinson projection). (b) A structural sketch of (a); the patera and main  
401 island are outlined in a solid blue and dotted black lines, respectively. The boundaries of the features  
402 we interpret to be extensional structures are shown with solid black lines. The units shown are from the  
403 Io global geological map (Williams et al., 2011). This scene is in azimuthal equidistant projection,  
404 centered at 13.2°N, 51.3°E.

405

406 **Figure 2.** A portion of Emakong Patera, which has straight edges (green arrows) that terminate at sharp  
407 corners (Radebaugh et al., 2001). The location of Emakong Patera is shown on the global Io mosaic.  
408 The main scene comprises Galileo SSI images 5000r, 5139r, and 5140r, and is in azimuthal equidistant  
409 projection, centered at 3.5°S, 240.0°E.

410

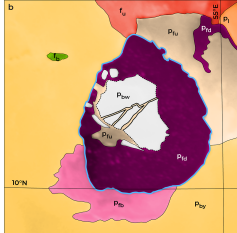
411 **Figure 3.** Hi'iaka Montes, examples of thrust fault-bounded mountain blocks on Io that show  
412 substantial evidence for extensional deformation (pink arrows). The blue arrow indicates a lava flow.  
413 The position of Hi'iaka Montes is shown on the global Io mosaic. The main scene comprises Galileo  
414 SSI images 7465r, 7478r, and 7500r, and is in azimuthal equidistant projection, centered at 4.5°S,  
415 279.0°E.

416

417 **Figure 4.** A schematic showing thrust faults (heavy black lines) dominating the lower part and  
418 extensional structures (thin black lines) throughout the upper part of Io's lithosphere. Example  
419 kinematic indicators are shown, as are magma bodies (examples marked by white arrows) and where

420 magma is ascending along normal faults (yellow arrows). The principal compressive stresses for the  
421 upper and lower lithosphere are also shown;  $\sigma_H$  and  $\sigma_h$  are horizontal stresses, and  $\sigma_V$  is the vertical  
422 stress. Where mountains are present, deep-seated thrusts extend to the surface (not shown here).





### UNITS

from Williams et al. (2011)

	$P_{bw}$	white bright plains material
	$P_{cy}$	yellow bright plains material
	$P_{fb}$	bright patera floor material
	$P_{fd}$	dark patera floor material
	$P_{fu}$	undivided patera floor material
	$f_b$	bright flow material
	$f_u$	undivided flow material
	$P_l$	layered plains material

	patera outline
	patera island outline
	extensional structure

Note: Units are not shown here in stratigraphic order.



